Ultramicroscopy 183 (2017) 84–88

Contents lists available at ScienceDirect

Ultramicroscopy

journal homepage: www.elsevier.com/locate/ultramic

Exploiting micro-scale structural and chemical observations in real time for understanding chemical conversion: LEEM/PEEM studies over CeO_x–Cu(111)

Tomáš Duchoň[a], Johanna Hackl[b], Jan Höcker[c], Kateřina Veltruská[a], Vladimír Matolín[a], Jens Falta[c,d], Stefan Cramm[b], Slavomír Nemšák[b], Claus M. Schneider[b], Jan Ingo Flege[c,d], Sanjaya D. Senanayake[e,*]

[a] Charles University, Faculty of Mathematics and Physics, Department of Surface and Plasma Science, V Holešovičkách 2, 18000 Prague 8, Czech Republic
[b] Peter Grünberg Institute (PGI-6), Forschungszentrum Jülich, 52425 Jülich, Germany
[c] Institute of Solid State Physics, University of Bremen, Otto-Hahn-Allee 1, 28359 Bremen, Germany
[d] MAPEX Center for Materials and Processes, University of Bremen, 28359 Bremen, Germany
[e] Chemistry Department, Brookhaven National Laboratory, Upton, NY 11973, United States

ARTICLE INFO

Article history:
Received 23 January 2017
Revised 31 March 2017
Accepted 9 May 2017
Available online 10 May 2017

Keywords:
Model systems
Length-scale
Defects
Ceria
Photoemission electron microscopy

ABSTRACT

Proper consideration of length-scales is critical for elucidating active sites/phases in heterogeneous catalysis, revealing chemical function of surfaces and identifying fundamental steps of chemical reactions. Using the example of ceria thin films deposited on the Cu(111) surface, we demonstrate the benefits of multi length-scale experimental framework for understanding chemical conversion. Specifically, exploiting the tunable sampling and spatial resolution of photoemission electron microscopy, we reveal crystal defect mediated structures of inhomogeneous copper–ceria mixed phase that grow during preparation of ceria/Cu(111) model systems. The density of the microsized structures is such that they are relevant to the chemistry, but unlikely to be found during investigation at the nanoscale or with atomic level investigations. Our findings highlight the importance of accessing micro-scale when considering chemical pathways over heteroepitaxially grown model systems.

1. Introduction

Contemporary heterogeneous catalysis takes advantage of a plethora of morphologically complex and often inhomogeneous materials enabled by advances in synthesis, fabrication and functionalization of nanostructures [1]. While these materials often provide superior atomic level insights into fundamental chemistry, including the atomic active sites, chemical and electronic state, the dynamic behavior under in situ or operando conditions is generally poorly understood. The primary obstacle of this is the inability to discriminate the fundamental steps of manifold chemical reactions proceeding over convoluted structural configurations of catalyst surfaces from single atoms to large terraces or even extended surfaces. A collective of processes prevails in chemical reactions, including adsorption, rapid reactant activation or diffusion, intermediate/transient species formation, product desorption and mass transport over surfaces. These reactions are often activated thermally or with other activators (electrostatic potential, photoexcitation). Model systems, especially when prepared in the form of thin epitaxial films, can be used to reduce this complexity and isolate the individual configurations that may provide invaluable information about the elementary reaction steps and atomistic insight on active chemistry [2]. Systematic experimentation with models of compositional or redox/chemical state changes can be performed with nearly perfect reproducibility to make unbiased comparisons and establish principles for chemical reactivity or catalytic activity [3,4]. A further benefit of this approach is the relative ease with which experimental data obtained from extended low-index surfaces can be coupled to theoretical calculations, most frequently performed using density functional theory (DFT) [5].

However, the utilization of model systems typically comes with several assumptions one has to be mindful of. Specifically, the supposition that the model system and its behavior is truly representative of an ideal low index surface is a strong one, and especially so when the available chemical and structural data from the system do not share the same length-scale, as is often the case. The most common methods used for chemical analysis average over ar-

* Corresponding author.
E-mail address: ssenanay@bnl.gov (S.D. Senanayake).

http://dx.doi.org/10.1016/j.ultramic.2017.05.003
0304-3991/

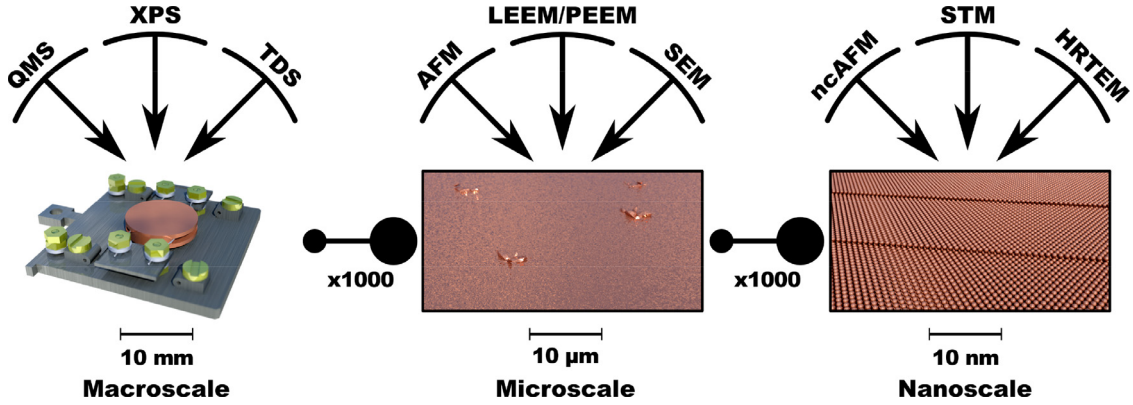

Fig. 1. Schematic representation of the length-scale of various characterization techniques. The importance of the microscale information is highlighted by the possibility to miss relevant microsized structures on the surface.

eas in the order of µm to mm, while structural analysis that can support the above-mentioned assumption has to resolve features in the order of nm and less. Thus it is, for example, possible to carefully combine scanning tunneling microscopy (STM) with DFT [6], but conjoining the two with x-ray photoelectron spectroscopy (XPS) can lead one to draw conclusions that may not correlate with spatial averaged structural and chemical information [7]. The length-scale challenge is schematically depicted in Fig. 1. In this contribution, we will introduce a new way to exploit real time chemical and structural understanding of the model system approach by employing combined low energy electron microscopy (LEEM), diffraction (LEED) and photoemission electron microscopy (PEEM), techniques which allow characterizing the surface structure and chemistry on the same length-scale [8], in the study of ceria/Cu(111) model system, which has recently appeared in many physico-chemical studies [9].

2. Methods and materials

Experiments were carried out in two separate LEEM instruments with a base pressure of 1×10^{-8} Pa: A commercial Elmitec LEEM-III and a FE-LEEM P90 instrument commercialized by SPECS. The FE-LEEM P90 is a permanent end station at the Research Center Jülich soft x-ray beamline UE56/1-SGM of the synchrotron facility BESSY II, Berlin, Germany, enabling the use of LEEM, μ-LEED and XAS-PEEM. Samples were prepared using identical growth procedures in both instruments. The Cu(111) single crystals (MaTecK) were cleaned by several cycles of Ar^+ sputtering (1.5 keV) and annealing in vacuum at 600 °C. The cycles were interspaced by annealing in 5×10^{-5} Pa of oxygen at 600 °C, which has proved to be an effective way of forcing cerium atoms dissolved in the top part of the copper crystal (from prior ceria experiments) to the surface, where they can be more effectively cleaned by successive sputtering. Cerium was evaporated from an e-beam source in oxygen ambience (partial pressure ranging from 5×10^{-5} to 2×10^{-4} Pa) at 450 °C.

3. Results and discussion

The ceria/Cu(111) system has been the focus of numerous chemical reactivity studies and has been extensively characterized by ion spectroscopy scattering (ISS), infrared spectroscopy (IR), XPS, low energy electron diffraction (LEED), STM, LEEM and modelled theoretically in the framework of DFT [4,9,10]. The growth of ceria on Cu(111) has been thought of as a simple diffusion limited process that results in the formation of CeO_x(111) epitaxial layers due to the nearly perfect 1.5 lattice coincidence with the substrate [11]. However, a recent discovery of the simultaneous nucleation of

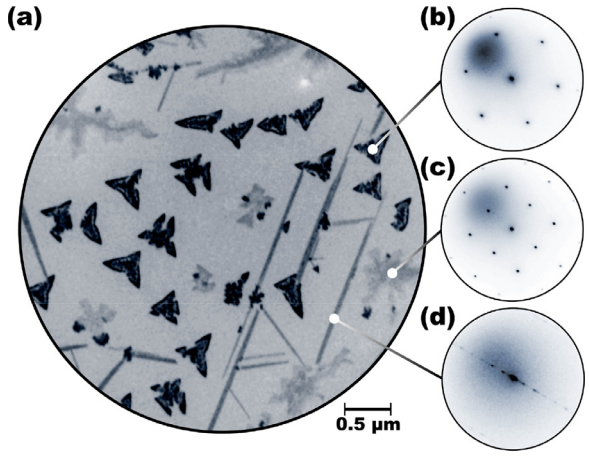

Fig. 2. Various microscale phases of ceria growing on the Cu(111) surface at 450 °C in 5×10^{-7} Pa of O_2. (a) A 5 µm field of view LEEM image recorded at primary electron energy (E_p) of 5.2 eV, local LEED patterns of (b) a triangular CeO_x(111) island ($E_p = 36$ eV), (c) a dendritic CeO_x(100) island ($E_p = 36$ eV) and (d) a needle-like ceria structure ($E_p = 17$ eV).

various ceria phases on the Cu(111) surface (see Fig. 2) has clearly shown the established principles of growth to be overly simplistic [12,13]. Given that there is no general theory of oxide nucleation at the atomic scale, one has to carefully account for all the thermodynamic variables influencing the growth, most importantly the temperature and chemical potential of the present chemical elements and molecules. The surface oxygen chemical potential plays a decisive role in the formation of ceria layers exposing either the (111) or (100) surface, as observed in the case of ceria/Cu(111) [12]. This structural heterogeneity of models is likely to be a major influence to the subsequent titration of chemical reactivity and also catalytic activity.

While relevant growth conditions or preparation parameters are typically provided in manuscripts, their variance can be considerable. This is especially important for the oxygen pressure used during the growth of ceria, which can vary, depending on the type of gauge used and the geometry of the experimental setup, by more than an order of magnitude. Furthermore, the important parameter in ceria growth on Cu(111) is actually the surface oxygen chemical potential, which depends also on the Ce evaporation rate, a complex kinetic set of parameters. One can thus achieve conditions favorable to the nucleation of CeO_x(100) at the oxygen pressures typically used for preparation of CeO_x(111) by lowering the deposition rate and vice versa. Consequently, it is hard to transfer

such an experiment from one apparatus to another. For example, inferring from an STM experiment conducted using one apparatus the morphology of a sample prepared in a different one is difficult, even with a very high degree of experimental controls. Specifically, it is very hard to disprove the existence of a minority phase (i.e., $CeO_x(100)$ phase on a $CeO_x(111)$/Cu(111) sample) if such evidence cannot be observed by a conventional LEED apparatus. This in itself poses a major obstacle for the utilization of ceria/Cu(111) as a model system due to the chemistry of ceria being highly face and structure sensitive [14,15]. The issue of phase heterogeneity is not limited to the ceria/Cu(111), but extends to other established ceria model systems, such as ceria/Ru(0001), too [16].

Furthermore, variations in chemistry observed as a result of the presence of defects in the surface of the model catalyst can also be important. The existence of microscopic defects, or even visible ones — such as scratches or dents, on the single crystal surface is often ignored but can be the locale for rich chemistry. The common practice of carefully repeating preparation recipes may, although helpful in other ways, have unwanted or unnoticed side effects, e.g., increases in defect or step density. While this is absolutely fine for highly local measurements where a defect-free area of the sample is carefully chosen for the analysis, area averaging measurements, such as XPS or activity measurements obtained from a reactor, may be strongly influenced by the history of the crystal. One important solution is to look for in situ methods where length-scales are inclusive of large area effects in parallel with high resolution local area atomic probes, such as provided by LEEM/PEEM. Intensity-voltage (I(V)) LEEM exploits the material-specific variation of the specular reflectivity of low-energy electrons depending on kinetic energy [17], which owing to the underlying diffraction phenomena is largely determined by the local atomic structure of the sample. This way, I(V)-LEEM intrinsically provides mesoscale mappings representative of the local atomic structure with few nanometer and even temporal resolution (if dynamic I(V)-LEEM [17] is performed). However, the data is generally harder to interpret for complex structures of unknown chemical composition, suggesting the complementary use of (X-ray) PEEM in these cases.

Fig. 3 shows several examples of complex agglomerates growing at crystal defects in a Cu(111) single crystal during cerium evaporation in an oxygen background using PEEM. The lateral size of the structures shown in Fig. 3 can reach tens of micrometers, but the density depends highly on the quality of the single crystal surface. Based on the analysis of several single crystals from MaTecK, both brand new and a few years old ones, a 0.02–2% of the surface area can be reasonably expected to be covered by the defect mediated structures, depending on the sample history. In order to gauge the significance of the seemingly low coverage we draw a comparison between the concentration of observed defects and step edges, as an example of catalytically relevant sites. A 1% coverage equates to semi-infinite steps on vicinal surfaces separated by 20 nm or to steps on surfaces with average terrace area of 10,000 nm^2. Step edges of comparable concentrations have been previously shown to markedly affect chemical reactions [18–20]. Furthermore, our estimate does not take into account the actual surface area of the structures and can considerably undervalue their effect. Consequently, while the complicated morphology and low density will make observation of regions of interest in STM quite unlikely, their contribution to signals of area averaging techniques cannot be overlooked. Hence, the ability to observe such structures carefully in parallel with STM imaging is very important.

The approach to include multiple length-scales in the above example will enhance our understanding of the structure–reactivity relationship, while also allowing for a real-time observation of the chemical composition of the surface mediated structures. In addition, micro X-ray absorption spectroscopy (XAS) measurements can also reveal these structures to be an inhomogeneous, mixed Cu–O–Ce phase, with regions of varying ceria stoichiometry and copper content (see Fig. 4).

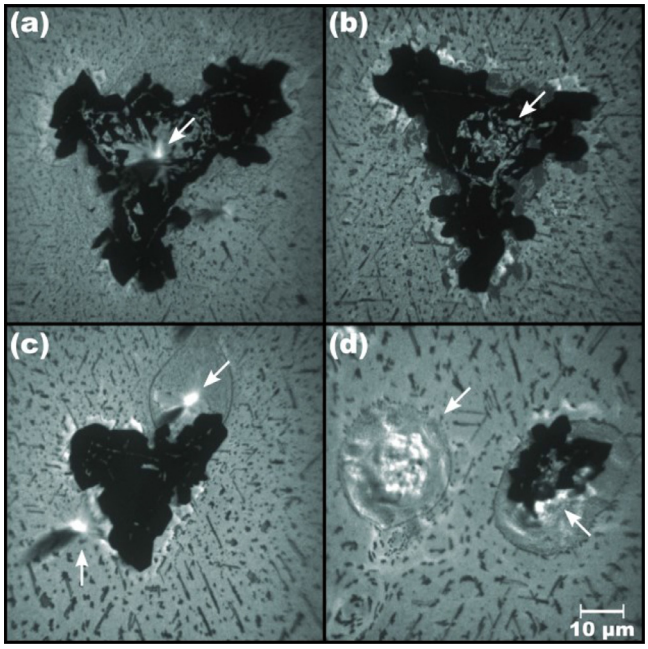

Fig. 3. PEEM images of ceria related structures growing (a), (b) over, (c) around and (d) inside crystal defects in a Cu(111) single crystal during cerium evaporation in 2×10^{-4} Pa of O_2 at 450 °C. White arrows highlight the position of crystal defects. The smaller elongated objects are $CeO_x(100)$ islands growing along substrate steps. The images were acquired using a mercury-arc lamp as a source of photons.

The measured Cu L_3 edge spectra (Fig. 4(b)) exhibit a two peak structure in the measured range, with maxima at 932.8 and 936.8 eV, characteristic for metallic copper. In fact, the spectra taken from regions A, C and D marked in Fig. 4(a) are practically identical to a reference spectrum of a clean copper single crystal (not shown). However, region B shows a prominent decrease of the second peak, which can be associated with the formation of copper oxide [21]. This could either mean that the copper is oxidized through a significant oxygen spillover from ceria, or that it forms a mixed oxide with ceria. We have mapped the loss of intensity of the second peak in real space by dividing a PEEM image taken at 932.8 eV by an image taken at 936.8 eV. The map shown in Fig. 4(c) reveals that the oxidized state is correlated with the defect mediated structure. Because we do not see oxidized copper around or below regular $CeO_x(100)$ and $CeO_x(111)$ islands even though oxygen is expected to be adsorbed on the surface in oxygen ambience in concentrations pertaining to the '29' and '44' Cu_xO structures [22,23], this strongly suggests the formation of a copper–ceria mixed oxide in the defect mediated structures.

The analysis of measured Ce M_5 edge spectra (Fig. 4(b)) further supports this hypothesis. Because occupation of the highly localized f level dramatically changes the X-ray absorption fingerprint of Ce atoms, one can use fitting procedures to determine stoichiometry of ceria from X-ray absorption spectra. A linear combination of referential Ce^{3+} and Ce^{4+} peaks [24] yields a stoichiometry of $CeO_{1.89 \pm 0.01}$, $CeO_{1.96 \pm 0.01}$, $CeO_{1.97 \pm 0.01}$ and $CeO_{1.80 \pm 0.01}$ for spectra from regions marked A, B, C and D in Fig. 4, respectively. While the spectra clearly illustrate the inhomogeneity of the defect mediated structure, a more significant finding is that the ceria retains its relatively high degree of reduction even in an oxygen ambient (5×10^{-7} Pa of O_2). This is consistent with the properties of a copper–ceria solid solution [25], which can, unlike pure ceria, preserve cerium atoms in a 3+ state even in oxygen ambient through

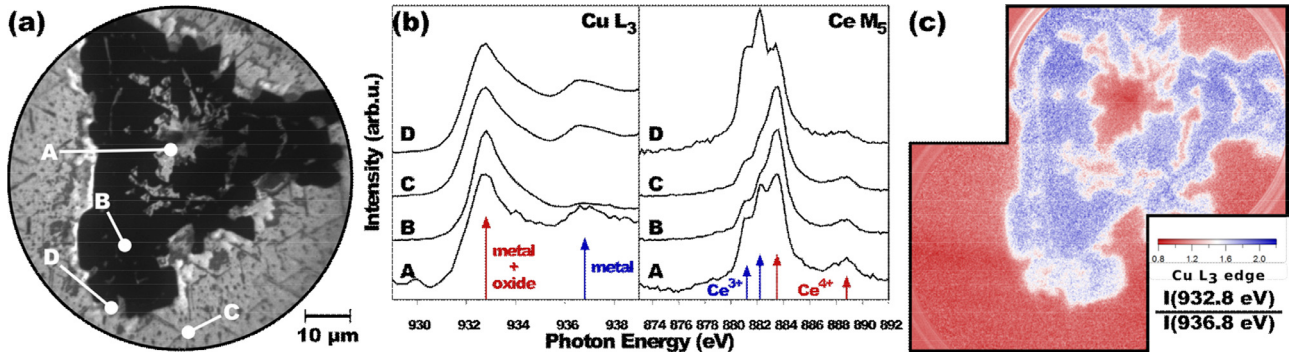

Fig. 4. XAS analysis of a defect mediated structure. (a) A mercury-arc lamp PEEM image. (b) XAS spectra of the Cu L_3 edge and Ce M_5 edge collected from regions marked in (a). The red and blue arrows indicate features of a specific chemical states. (c) Image map of the oxidation state of copper realized through a division of XAS-PEEM images collected at two characteristic energies of the Cu L_3 edge — 932.8 eV (oxide + metal) and 936.8 eV (metal).

electronic exchange with copper, i.e. by $Ce^{4+} + Cu^{1+} \rightarrow Ce^{3+} + Cu^{2+}$. It should be noted that a lower concentration of oxygen vacancies, such as the one in region C, can be ascribed either to height variations of the structures or charge compensation of the polar $CeO_x(100)$ surface [26].

The presence of the mixed oxide phase on the surface can have a huge impact on the chemical processes proceeding over the ceria/Cu(111) model systems as copper–ceria is a well-known catalyst utilized in several industrial processes, such as the water-gas shift reaction [27,28], preferential CO oxidation [29–31], methanol synthesis [4,32], and others [33]. In fact, our observations may even explain several variations between ceria model systems that have been reported in the literature. An example that clearly illustrates the issue is the interaction of the (111) plane of ceria with water. Adsorption of water on reduced CeO_x was shown to lead to further reduction of the ceria surface in the case of reduced $CeO_x(111)/Cu(111)$ [34] and oxidation of the ceria surface in the case of reduced $CeO_x(111)/Ru(0001)$ [35]. Furthermore, reduced $CeO_x(111)/Ru(0001)$ was reported to dissociate water, which lead to production of hydrogen at 600 K [36], but no such reaction was observed in the case of reduced $CeO_x(111)$ on yttria-stabilized $ZrO_2(111)$ [37]. Apart from the interaction with water, the ceria/Cu(111) model systems consistently exhibit a much richer chemistry in comparison with ceria/Ru(0001) model systems with respect to CO dissociation [38–40] and acetic acid decomposition [41,42]. Taking into account that copper oxide plays an active role in the above-mentioned reactions [29], it is noteworthy that the effects related to the presence of the defect mediated structures will not be subdued by increasing the film thickness, which may otherwise mitigate support related effects that arise from the difference between thin films and bulk-like systems.

4. Conclusions

Our findings draw attention to the importance of new in situ methods to probe the dynamic nature of surface chemistry in model surfaces for the understanding of fundamental steps of catalyzed chemical reactions. The ability to observe reactions at multiple length-scales highlights the importance for providing structural and chemical data at the appropriate length-scale when discussing chemistry of explicit structural features. Especially apparent is also the fact that microscale information, which is often disregarded in the transition from macroscale to nanoscale, should weigh in more heavily when interpreting data from model systems.

Acknowledgements

This work was supported by the U.S. Department of Energy, Office of Science, Office of Basic Energy Sciences, and Catalysis Science Program under contract No. DE-SC0012704. This work was also supported by the European COST Action CM1104, the Czech Science Foundation (GAČR 15-06759S) and the Grant Agency of Charles University (GAUK 472216).

References

[1] A. Tiwari, S. Titinchi, Advanced Catalytic Materials, John Wiley & Sons, Hoboken, NJ, USA, 2015.
[2] H.-J. Freund, Chem.–Eur. J. 16 (2010) 9384–9397.
[3] K. Mudiyanselage, S.D. Senanayake, L. Feria, S. Kundu, A.E. Baber, J. Graciani, A.B. Vidal, S. Agnoli, J. Evans, R. Chang, S. Axnanda, Z. Liu, J.F. Sanz, P. Liu, J.A. Rodriguez, D.J. Stacchiola, Angew. Chem. Int. Ed. 52 (2013) 5101–5105.
[4] J. Graciani, K. Mudiyanselage, F. Xu, A.E. Baber, J. Evans, S.D. Senanayake, D.J. Stacchiola, P. Liu, J. Hrbek, J.F. Sanz, J.A. Rodriguez, Science 345 (2014) 546–550.
[5] J. Paier, C. Penschke, J. Sauer, Chem. Rev. 113 (2013) 3949–3985.
[6] J.-F. Jerratsch, X. Shao, N. Nilius, H.-J. Freund, C. Popa, M.V. Ganduglia-Pirovano, A.M. Burow, J. Sauer, Phys. Rev. Lett. 106 (2011) 246801.
[7] G.N. Vayssilov, Y. Lykhach, A. Migani, T. Staudt, G.P. Petrova, N. Tsud, T. Skála, A. Bruix, F. Illas, K.C. Prince, V. Matolín, K.M. Neyman, J. Libuda, Nat. Mater. 10 (2011) 310–315.
[8] D.C. Grinter, S.D. Senanayake, J.I. Flege, Appl. Catal. B Environ. 197 (2016) 286–298.
[9] D.R. Mullins, Surf. Sci. Rep. 70 (2015) 42–85.
[10] J.A. Rodriguez, J. Graciani, J. Evans, J.B. Park, F. Yang, D. Stacchiola, S.D. Senanayake, S. Ma, M. Pérez, P. Liu, J. Fdez Sanz, J. Hrbek, Angew. Chem. Int. Ed. 48 (2009) 8047–8194.
[11] T. Staudt, Y. Lykhach, L. Hammer, M.A. Schneider, V. Matolín, J. Libuda, Surf. Sci. 603 (2009) 3382–3388.
[12] J. Höcker, T. Duchoň, K. Veltruská, V. Matolín, J. Falta, S.D. Senanayake, J.I. Flege, J. Phys. Chem. C 120 (2016) 4895–4901.
[13] O. Stetsovych, J. Beran, F. Dvořák, K. Mašek, J. Mysliveček, V. Matolín, Appl. Surf. Sci. 285 (2013) 766–771.
[14] G. Vilé, S. Colussi, F. Krumeich, A. Trovarelli, J. Pérez-Ramírez, Angew. Chemie Int. Ed. 53 (2014) 12069–12072.
[15] D.R. Mullins, P.M. Albrecht, F. Calaza, Top. Catal. 56 (2013) 1345–1362.
[16] J.I. Flege, J. Höcker, B. Kaemena, T.O. Menteş, A. Sala, A. Locatelli, S. Gangopadhyay, J.T. Sadowski, S.D. Senanayake, J. Falta, Nanoscale 8 (2016) 10849–10856.
[17] J.I. Flege, E.E. Krasovskii, Phys. Status Solidi–Rapid Res. Lett. 8 (2014) 463–477.
[18] B.L.M. Hendriksen, M.D. Ackermann, R. van Rijn, D. Stoltz, I. Popa, O. Balmes, A. Resta, D. Wermeille, R. Felici, S. Ferrer, J.W.M. Frenken, Nat. Chem. 2 (2010) 730–734.
[19] O. Balmes, G. Prevot, X. Torrelles, E. Lundgren, S. Ferrer, ACS Catal. 6 (2016) 1285–1291.
[20] B. Eren, D. Zherebetskyy, L.L. Patera, C.H. Wu, H. Bluhm, C. Africh, L.-W. Wang, G.A. Somorjai, M. Salmeron, Science 351 (2016) 475–478.
[21] M. Grioni, J.F. van Acker, M.T. Czyżyk, J.C. Fuggle, Phys. Rev. B 45 (1992) 3309–3318.
[22] A.J. Therrien, R. Zhang, F.R. Lucci, M.D. Marcinkowski, A. Hensley, J.-S. McEwen, E.C.H. Sykes, J. Phys. Chem. C 120 (2016) 10879–10886.
[23] F. Jensen, F. Besenbacher, I. Stensgaard, Surf. Sci. 269–270 (1992) 400–404.
[24] J. Höcker, T.O. Menteş, A. Sala, A. Locatelli, T. Schmidt, J. Falta, S.D. Senanayake, J.I. Flege, Adv. Mater. Interfaces 2 (2015) 1500314.
[25] S. Hočevar, J. Batista, J. Levec, J. Catal. 184 (1999) 39–48.
[26] Y. Pan, N. Nilius, C. Stiehler, H.-J. Freund, J. Goniakowski, C. Noguera, Adv. Mater. Interfaces 1 (2014) 1400404.
[27] X. Wang, J.A. Rodriguez, J.C. Hanson, D. Gamarra, A. Martínez-Arias, M. Fernández-García, J. Phys. Chem. B 110 (2006) 428–434.
[28] S.Y. Yao, W.Q. Xu, A.C. Johnston-Peck, F.Z. Zhao, Z.Y. Liu, S. Luo, S.D. Senanayake, A. Martínez-Arias, W.J. Liu, J.A. Rodriguez, Phys. Chem. Chem. Phys. 16 (2014) 17183–17195.

[29] F. Wang, R. Büchel, A. Savitsky, M. Zalibera, D. Widmann, S.E. Pratsinis, W. Lubitz, F. Schüth, ACS Catal 6 (2016) 3520–3530.
[30] S.D. Senanayake, D. Stacchiola, J.A. Rodriguez, Acc. Chem. Res. 46 (2013) 1702–1711.
[31] S. Yao, K. Mudiyanselage, W. Xu, A.C. Johnston-Peck, J.C. Hanson, T. Wu, D. Stacchiola, J.A. Rodriguez, H. Zhao, K.A. Beyer, K.W. Chapman, P.J. Chupas, A. Martínez-Arias, R. Si, T.B. Bolin, W. Liu, S.D. Senanayake, ACS Catal. 4 (2014) 1650–1661.
[32] S.D. Senanayake, P.J. Ramírez, I. Waluyo, S. Kundu, K. Mudiyanselage, Z. Liu, Z. Liu, S. Axnanda, D.J. Stacchiola, J. Evans, J.A. Rodriguez, J. Phys. Chem. C 120 (2016) 1778–1784.
[33] T. Montini, M. Melchionna, M. Monai, P. Fornasiero, Chem. Rev. 116 (2016) 5987–6041.
[34] V. Matolín, I. Matolínová, F. Dvořák, V. Johánek, J. Mysliveček, K.C. Prince, T. Skála, O. Stetsovych, N. Tsud, M. Václavů, B. Šmíd, Catal. Today 181 (2012) 124–132.
[35] D.R. Mullins, P.M. Albrecht, T. Chen, F.C. Calaza, M.D. Biegalski, H.M. Christen, S.H. Overbury, J. Phys. Chem. C 116 (2012) 19419–19428.
[36] L. Kundakovic, D.R. Mullins, S.H. Overbury, Surf. Sci. 457 (2000) 51–62.
[37] M.A. Henderson, C.L. Perkins, M.H. Engelhard, S. Thevuthasan, C.H.F. Peden, Surf. Sci. 526 (2003) 1–18.
[38] D. Mullins, K. Zhang, Surf. Sci. 513 (2002) 163–173.
[39] M. Happel, J. Mysliveček, V. Johánek, F. Dvořák, O. Stetsovych, Y. Lykhach, V. Matolín, J. Libuda, J. Catal. 289 (2012) 118–126.
[40] A. Neitzel, Y. Lykhach, T. Skála, N. Tsud, M. Vorokhta, D. Mazur, K.C. Prince, V. Matolín, J. Libuda, Phys. Chem. Chem. Phys. 16 (2014) 24747–24754.
[41] F.C. Calaza, T.-L. Chen, D.R. Mullins, Y. Xu, S.H. Overbury, Catal. Today 253 (2015) 65–76.
[42] A. Neitzel, Y. Lykhach, V. Johánek, N. Tsud, T. Skála, K.C. Prince, V. Matolín, J. Libuda, J. Phys. Chem. C 119 (2015) 13721–13734.